Proceedings of the 2025 SICE Festival with Annual Conference
September 9-12, 2025, Chiang Mai, Thailand

Transition Motion Trajectory from Wheeled-Legged Locomotion to Rolling Locomotion for Mobile Quad-arm Robot

Yuika Yoshimoto[1†], Jun Watanabe[2], Zhaoyang Huang[3], and Hisayoshi Muramatsu[1]

[1]Mechanical Engineering Program, Hiroshima University, Higashihiroshima 739-8527, Japan
(Tel: +81-82-424-7575; E-mail: muramatsu@hiroshima-u.ac.jp)
[2]Mechanical Engineering Department, Mitsubishi Heavy Industries Machinery Systems, Mihara 729-0393, Japan
(E-mail: watanabet227@gmail.com)
[3]Department of Robotics, Graduate School of Engineering, Tohoku University, Sendai 980-8579, Japan
(E-mail: zhaoyang.r.huang@gmail.com)

Abstract: Mobile robots that have an ability to run through various environments can help people to avoid dangerous situations, such as exploring a disaster area. In order to adapt to various environments, hybrid mobile robots that combine multiple locomotion and select the locomotion according to the terrain have been developed. However, there are no hybrid mobile robots that combine wheeled, wheeled-legged, and rolling locomotion. In this study, we developed a mobile quad-arm robot equipped with wheeled, wheeled-legged, and rolling locomotion capabilities, and proposed and verified a motion trajectory for the transition from wheeled-legged locomotion to rolling locomotion. The developed robot transits from the wheeled-legged posture to the rolling posture using four arms with different configurations and then rolls. The proposed motion trajectory was verified in the experiment where the robot achieved rolling locomotion. The experiments also verified the wheeled and wheeled-legged locomotion capabilities.

Keywords: Hybrid robot, mobile robot, hybrid locomotion, rolling locomotion, motion trajectory

1. INTRODUCTION

Mobile robots are expected to have an ability to run through various environments and dangerous areas instead of people. For mobile robots to adapt to various environments, it is effective to have multiple locomotion and select locomotion according to the environment. Therefore, hybrid mobile robots that combine multiple locomotion have been developed.

Robosimian [1], ANYmal [2], and CENTAURO [3] possess legged and wheeled locomotion capabilities. Legged locomotion and wheeled locomotion are suitable at locomotion in uneven terrain and even terrain, respectively. For loco-manipulation that unifies locomotion and manipulation, Robosimian [1] and ALPHERD [4] were also developed. Scorpio [5] is a hybrid mobile robot with crawling, rolling, and wall-climbing locomotion capabilities. Rolling locomotion excels at locomotion downhill because they can continue to move without driving a motor while descending. The snake-like robot [6] achieved to unify snake and rolling locomotion. ARMS [7], which was developed in our previous research, combines wheeled locomotion, wheeled-legged locomotion, and loco-manipulation capabilities with a reduced number of actuators. In this way, Hybrid mobile robots can adapt to several environments and do tasks in contrast to a robot with only one specific capability. However, there are no hybrid mobile robots that combine wheeled, wheeled-legged, and rolling locomotion.

This study developed a hybrid quad-arm robot that combines wheeled, wheeled-legged, and rolling locomotion. Using the robot, this paper proposes a motion trajectory for transition from wheeled-legged locomotion

† Yuika Yoshimoto is the presenter of this paper.

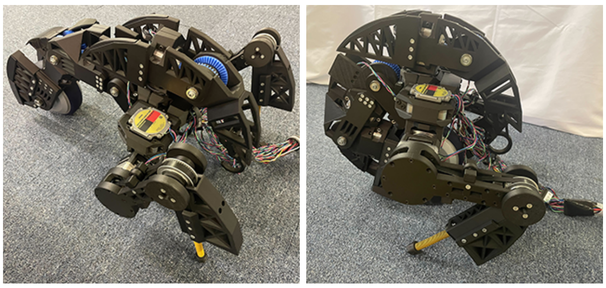

(a) (b)

Fig. 1: Quad-arm robot. (a) Wheeled-legged posture. (b) Rolling posture.

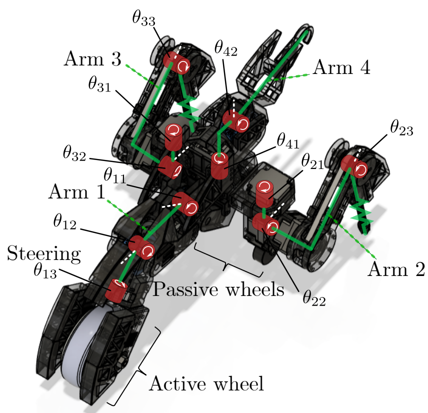

Fig. 2: Configuration of quad-arm robot. The red cylinders indicate the joints. The white arrows in the cylinders correspond to the positive angle direction. The dotted white lines are the datum lines for the joint angles.

to rolling locomotion, which was verified in the experiment. Fig. 1 shows the developed quad-arm robot in

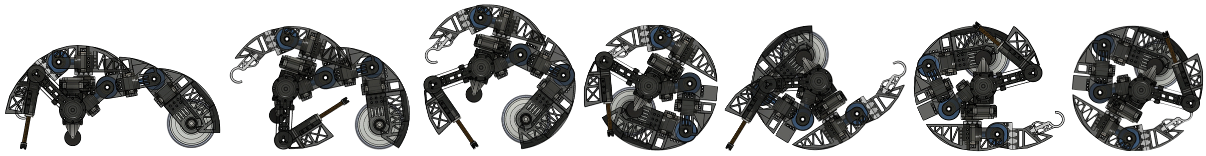

(a) $S_k = 0$. (b) $S_k = 1$. (c) $S_k = 2$. (d) $S_k = 3$. (e) $S_k = 4$. (f) $S_k = 5$. (g) $S_k = 6$.

Fig. 3: Posture at each step S_k for transition from wheeled-legged posture to rolling posture. The posture when $\mathrm{A}_2 = 150$ deg and $\mathrm{A}_3 = 55$ deg in the step $S_k = 4$ is shown in (e).

the wheeled-legged and rolling postures. The robot is equipped with 12 actuators, which is the same as that of ARMS [7]. Two experiments were conducted to verify the proposed motion trajectory and locomotion capabilities of the robot. In the wheeled and wheeled-legged locomotion experiment, the robot moved on even terrain by wheeled locomotion and climbed a slope by wheeled-legged locomotion. In the rolling locomotion experiment, the robot transited from wheeled-legged posture to rolling posture and descended a slope.

2. ROLLING MECHANISM DESIGN

Fig. 2 shows the configuration of the robot: a front arm (Arm 1), two rear arms (Arms 2 and 3), a back arm (Arm 4), a torso, an active wheel, and two passive wheels. The active wheel is attached to the tip of Arm 1, and the passive wheels are attached to the base of Arms 2 and 3, respectively. Arm 1 has three DOFs. One of them is for steering, and the others are rotated by transmitting the rotation of the motor using bevel gears. Arms 2 and 3 are equipped with a spring to absorb shock and an end-effector that can be designed depending on the purpose. The timing pulleys and timing belts are adopted to drive θ_{23} and θ_{33}. These three DOFs arms have a symmetrical structure. Arm 4 also has an end-effector for manipulation. This arm has two DOFs, and one of which uses bevel gears as same as that of Arm 1. The gear ratio of all bevel gears used in the robot is three. As mentioned above, the robot has 12 actuators for 11 joints and the active wheel. The robot's total weight is 13.35 kg. The height of the robot in the rolling posture is 0.36 m, and the width is 0.43 m.

The robot was designed to combine wheeled, wheeled-legged, and rolling locomotion capabilities without increasing the number of actuators from 12. For wheeled locomotion, the active wheel at the tip of Arm 1 and two passive wheels are used. For wheeled-legged locomotion, the wheel at Arm 1 is used as a passive wheel, and Arms 2 and 3 are used as legs. The transitions from wheeled-legged locomotion to wheeled locomotion and from wheeled locomotion to wheeled-legged locomotion are possible simply by rotating the second joints from the base of Arms 2 and 3 (θ_{22} and θ_{32}). For rolling locomotion, the robot needs to form a circle when viewed from the side. Therefore, the components that configure the robot are designed to have curves. These components for rolling locomotion are designed to reduce weight without compromising strength. These designs do not collide in each locomotion posture.

Two-Phase stepping motors (PKP262FD15AW-H100S from ORIENTAL MOTOR CO., LTD.) and corresponding drivers (CVD215BR-K from ORIENTAL MOTOR CO., LTD.) were employed as actuators for driving all joints. In-wheel motor (CAIW-80BA from Shinano Kenshi Co., Ltd.) and corresponding driver (PDBA-80B from Shinano Kenshi Co., Ltd.) were employed as the active wheel and actuator for driving the active wheel.

3. TRANSITION MOTION TRAJECTORY

For the transition from the wheeled-legged posture to the rolling posture, the robot takes six steps as shown in Fig. 3. The robot takes through these steps from left to right in Fig. 3. According to the index $k \in \mathbb{Z}_{\geq 0}$, step S_k is determined as

$$S_k = \begin{cases} 0 & \text{if } kT = 0 \text{ s} \\ 1 & \text{if } 0 \text{ s} < kT < 38 \text{ s} \\ 2 & \text{if } 38 \text{ s} \leq kT < 58 \text{ s} \\ 3 & \text{if } 58 \text{ s} \leq kT < 78 \text{ s} \\ 4 & \text{if } 78 \text{ s} \leq kT < 211 \text{ s} \\ 5 & \text{if } 211 \text{ s} \leq kT < 243 \text{ s} \\ 6 & \text{if } 243 \text{ s} \leq kT, \end{cases} \quad (1)$$

where T [s] denotes the sampling. The step $S_k = 0$ corresponds to the initial posture, which is the wheeled-legged posture. The first step $S_k = 1$ is to bring the tip of Arm 1 closer to the torso. The next step $S_k = 2$ is to put the curved part at the tip of Arm 1 on the ground. At step $S_k = 3$, Arm 1 gets in the rolling posture. After Arm 1 gets in the rolling posture, at step $S_k = 4$, the robot rolls forward by kicking the ground using Arms 2 and 3 as shown in Fig. 3(e) until it stops as shown in Fig. 3(f). At step $S_k = 5$, the robot does not descend and gets in the rolling posture except for the second joint of Arm 4. At the last step $S_k = 6$, the robot starts descending a slope by getting Arm 4 in the rolling posture. While descending a slope, the robot keeps the rolling posture as shown in Fig. 3(g). This method eliminates the need to drive motors to give the robot momentum for starting to descend.

The motor target angles $\theta_{ij,k}^{\mathrm{cmd}}$ [deg] change depending

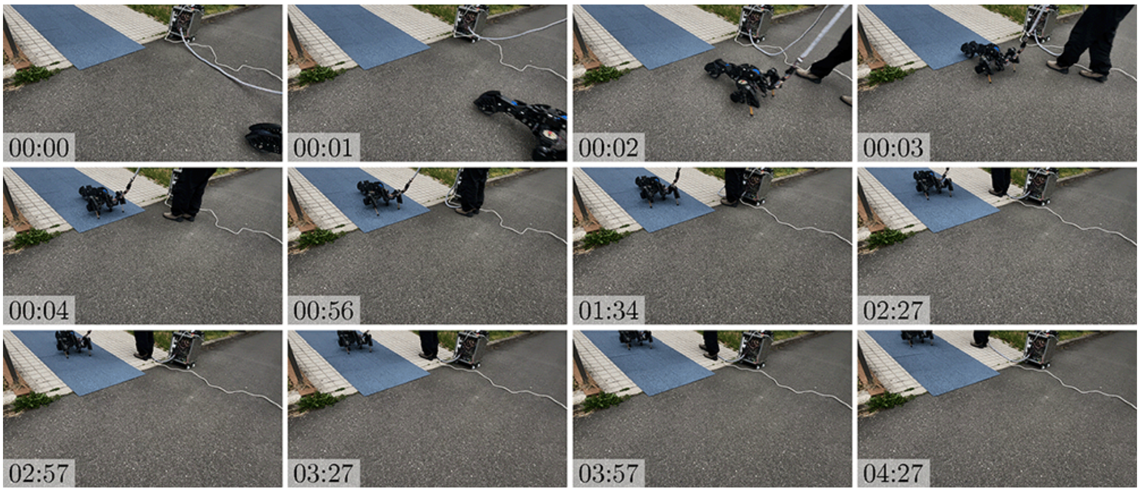

Fig. 4: Wheeled and wheeled-legged locomotion result.

on S_k as

$$\begin{bmatrix} \theta^{\rm cmd}_{11,k} \\ \theta^{\rm cmd}_{21,k} \\ \theta^{\rm cmd}_{22,k} \\ \theta^{\rm cmd}_{23,k} \\ \theta^{\rm cmd}_{32,k} \\ \theta^{\rm cmd}_{33,k} \\ \theta^{\rm cmd}_{42,k} \end{bmatrix} = \begin{cases} [\,90\ -180\ 45\ -125\ -45\ 125\ -390\,]^\top & \text{if } S_k = 0 \\ [\,30\ -285\ -105\ -125\ 105\ 125\ -390\,]^\top & \text{if } S_k = 1 \\ [\,150\ -315\ -35\ -105\ 35\ 105\ -390\,]^\top & \text{if } S_k = 2 \\ [\,315\ -315\ 0\ -125\ 0\ 125\ -390\,]^\top & \text{if } S_k = 3 \\ [\,315\ -315\ -\mathrm{A}_2\ -\mathrm{A}_3\ \mathrm{A}_2\ \mathrm{A}_3\ -270\,]^\top & \text{if } S_k = 4 \\ [\,315\ -315\ -30\ -125\ 30\ 125\ -270\,]^\top & \text{if } S_k = 5 \\ [\,315\ -315\ -30\ -125\ 30\ 125\ -390\,]^\top & \text{if } S_k = 6, \end{cases} \tag{2a}$$

$$\theta^{\rm cmd}_{13,k} = 0,\ \theta^{\rm cmd}_{21,k} = 0,\ \theta^{\rm cmd}_{31,k} = 0,\ \theta^{\rm cmd}_{41,k} = 0, \tag{2b}$$

where

$$\begin{bmatrix} \mathrm{A}_2 \\ \mathrm{A}_3 \end{bmatrix} = \begin{cases} [\ 0\quad 105\ ]^\top & \text{if } 78\ \mathrm{s} \le kT < 88\ \mathrm{s} \\ [\ -20\quad 125\ ]^\top & \text{if } 88\ \mathrm{s} \le kT < 98\ \mathrm{s} \\ [\ 35\quad 125\ ]^\top & \text{if } 98\ \mathrm{s} \le kT < 109\ \mathrm{s} \\ [\ 45\quad 100\ ]^\top & \text{if } 109\ \mathrm{s} \le kT < 125\ \mathrm{s} \\ [\ 50\quad 125\ ]^\top & \text{if } 125\ \mathrm{s} \le kT < 133\ \mathrm{s} \\ [\ 70\quad 115\ ]^\top & \text{if } 133\ \mathrm{s} \le kT < 143\ \mathrm{s} \\ [\ 70\quad 100\ ]^\top & \text{if } 143\ \mathrm{s} \le kT < 146\ \mathrm{s} \\ [\ 90\quad 125\ ]^\top & \text{if } 146\ \mathrm{s} \le kT < 158\ \mathrm{s} \\ [\ 150\quad 55\ ]^\top & \text{if } 158\ \mathrm{s} \le kT < 178\ \mathrm{s} \\ [\ 150\quad 95\ ]^\top & \text{if } 178\ \mathrm{s} \le kT < 203\ \mathrm{s} \\ [\ 150\quad 80\ ]^\top & \text{if } 203\ \mathrm{s} \le kT < 211\ \mathrm{s}. \end{cases} \tag{3}$$

Eq. (3) expresses the target angle for the kicking movement of Arms 2 and 3 in $S_k = 4$. In this trajectory, Arms 2 and 3 not only kick the ground for rolling forward, but also prevent the robot from rolling backward. From $kT = 78$ s, the robot spreads Arm 4 by driving the second joint (θ_{42}) as shown in Fig. 3(e). This Arm 4 prevents the robot from descending. Namely, at step $S_k = 4$, the robot descends forward using Arms 2 and 3 until it is stopped owing to Arm 4 as shown in Fig. 3(f).

According to $\theta^{\rm cmd}_{ij,k}$, the target pulse $P^{\rm cmd}_{ij,k} \in \mathbb{Z}$ is calculated as

$$P^{\rm cmd}_{ij,k} = \mathrm{sgn}\left(\frac{\theta^{\rm cmd}_{ij,k} - \theta^{\rm cmd}_{ij,0}}{p}\right) \max\left\{ n \in \mathbb{Z} \,\middle|\, n \le \left|\frac{\theta^{\rm cmd}_{ij,k} - \theta^{\rm cmd}_{ij,0}}{p}\right| \right\}, \tag{4}$$

where p denotes the angle per pulse 0.018 [deg/pulse]. To realize $P^{\rm cmd}_{ij,k}$, the controller sends a single pulse $\mathrm{sgn}(P^{\rm cmd}_{ij,k} - P_{ij,k-1})$ to each motor driver at each control loop, where

$$P_{ij,k} = P_{ij,k-1} + \mathrm{sgn}\left(P^{\rm cmd}_{ij,k} - P_{ij,k-1}\right). \tag{5}$$

Note that the function sgn is a sign function. Assume that negative pulse $P_{ij,k} < 0$ sends its pulse $|P_{ij,k}|$ in the negative direction.

4. EXPERIMENTS

Two experiments were conducted to verify the robot's locomotion capabilities and proposed motion trajectory. In both experiments, an slope where rugs were placed was used. The gradient of the slope is about five degrees.

Wheeled and wheeled-legged locomotion was verified, as shown in Fig. 4. The developed robot moved forward in the even terrain using the active wheel at the tip of Arm 1 and two passive wheels at the base of Arms 2 and 3. The velocity of the active wheel was commanded as 15.9 rad/s. Then, the robot walked using the three arms: Arms 1, 2, and 3. The active wheel was used as a passive wheel during walking. Arms 2 and 3 alternately pushed off the ground to go up the slope. The wheeled and wheeled-legged locomotion capabilities of the robot were validated.

Rolling locomotion was verified, as shown in Fig. 5. From 0 s to 270 s, Arms 1, 2, and 3 took the rolling posture from the wheeled-legged posture. From 211 s to 270

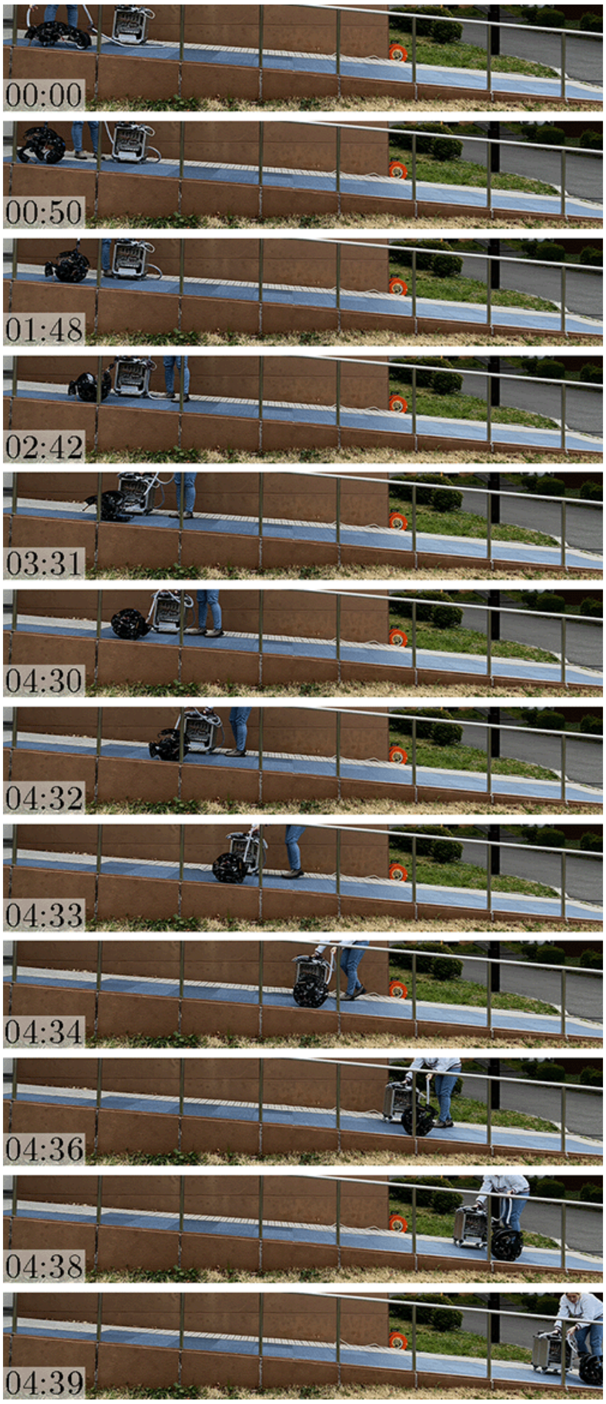

Fig. 5: Rolling locomotion result.

s, Arm 4 prevented the robot from descending the slope until Arms 2 and 3 got in the rolling posture. Then, the robot started to descend the slope from 270 s. The proposed motion trajectory and rolling locomotion capability of the robot were thus validated.

5. CONCLUSION

Motion trajectory for transition from wheeled-legged locomotion to rolling locomotion was proposed in this paper. Proposed motion trajectory was verified using the quad-arm robot that combines wheeled, wheeled-legged, and rolling locomotion with fewer actuators. This paper provided the mechanical design of the robot, rolling motion trajectory, and experiments of wheeled, wheeled-legged, and rolling locomotion. The robot achieved these three types of locomotion with only 12 actuators. In the experiments, the proposed motion trajectory and locomotion capabilities were validated: wheeled locomotion at even terrain, wheeled-legged locomotion at upward slope, and rolling locomotion at downward slope.

ACKNOWLEDGMENT

This work was supported by the Nagamori Foundation, Japan.

REFERENCES

[1] P. Hebert, M. Bajracharya, J. Ma, N. Hudson, A. Aydemir, J. Reid, C. Bergh, J. Borders, M. Frost, M. Hagman, J. Leichty, P. Backes, B. Kennedy, P. Karplus, B. Satzinger, K. Byl, K. Shankar, and J. Burdick, "Mobile manipulation and mobility as manipulation–design and algorithms of RoboSimian," Journal of Field Robotics, Vol.32, No.2, pp. 255-274, 2015.

[2] V. S. Medeiros, E. Jelavic, M. Bjelonic, R. Siegwart, M. A. Meggiolaro, and M. Hutter, "Trajectory optimization for wheeled-legged quadrupedal robots driving in challenging terrain," IEEE Robotics and Automation Letters, Vol.5, No.3, pp. 4172-4179, 2020.

[3] N. Kashiri, L. Baccelliere, L. Muratore, A. Laurenzi, Z. Ren, E. M. Hoffman, M. Kamedula, G. F. Rigano, J. Malzahn, S. Cordasco, P. Guria, A. Margan, and N. G. Tsagarakis, "CENTAURO: A hybrid locomotion and high power resilient manipulation platform," IEEE Robotics and Automation Letters, Vol.4, No.2, pp. 1595-1602, 2019.

[4] J. Hooks, M. S. Ahn, J. Yu, X. Zhang, T. Zhu, H. Chae, and D. Hong, "ALPHRED: A multi-modal operations quadruped robot for package delivery applications," IEEE Robotics and Automation Letters, Vol.5, No.4, pp. 5409-5416, 2020.

[5] T. Yanagida, R. Elara Mohan, T. Pathmakumar, K. Elangovan, and M. Iwase, "Design and implementation of a shape shifting rolling–crawling–wall-climbing robot," Applied Sciences, Vol.7, No.4, p. 342, 2017.

[6] A. Yamano, Y. Ikeda, K. Imai, and M. Chiba, "Efficient rolling motion for snake-like robots utilizing center of gravity shift," Mechatronics, Vol.94, p. 103024, 2023.

[7] H. Muramatsu, K. Kitagawa, J. Watanabe, Y. Yoshimoto, and R. Hisashiki, "A mobile quad-arm robot arms: Wheeled-legged tripedal locomotion and quad-arm loco-manipulation," Vol.37, No.2, 2025.